



# The Multifractal Detrended Fluctuation Analysis (Mf-Dfa) and Anomalies in Geomagnetic Total Field Intensity Prior To Mw~5.5 Earthquake

Timangshu Chetia, Saurabh Baruah\*, Chandan Dey, Santanu Baruah & Sangeeta Sharma

Geoscience & Technology Division, CSIR-North East Institute of Science & Technology, Jorhat-785 006, Assam, India

Received 28 May 2019; accepted 3 February 2022

In the research article, we report the anomalies observed in geomagnetic total field intensity ( $B_{\text{Total}}$ ) prior to Mw 5.5 Kokrajhar event. The multifractal analysis was scrutinized to reveal the underlying dynamics in the Geomagnetic Total field intensity time series. The multifractal spectrum on the day when the event occurred ( $T_{\text{Event day}}$ ) and its surrogate ( $T_{\text{Surrogate}}$ ) was investigated to understand the behavior and dynamics hidden in  $B_{\text{Total}}$  time series. A significant variation in the multifractal spectrum was observed between  $T_{\text{Day one}}$  (multifractal spectrum a day prior to the event) and  $T_{\text{Event day}}$ . It was also observed that the multifractality of  $B_{\text{Total}}$  when the event occurred ( $T_{\text{Event day}}$ ) got stronger than the multifractality of  $T_{\text{Day one}}$  and was sourced from low values distribution. The multifractality in  $T_{\text{Day one}}$  and  $T_{\text{Event day}}$  time series was not from source type long range correlation or sourced from broad probability density function. The investigation also manifests some non-linear features which probably evinces the anomalies to be seismic induced. The observations are elaborately emphasized in the article. The study scrutinizes the underlying dynamics in geomagnetic field intensity time series for earthquake precursory and forecast studies.

**Keywords:** Multifractal, Iterated amplitude adjust fourier transform, Geomagnetic field, Earthquake, Anomalies

## 1 Introduction

The North-eastern (NE) region of India is highly vulnerable to earthquake and lies in seismic zone V as per seismic zoning map of India<sup>1</sup>. The frequent occurrence of earthquakes in NE, India facilitates the probability of finding precursory phenomena which may lead for a successful forecast in near future. With these objectives, a Multiparametric Geophysical Observatory (MPGO) in Ouguri Hills (Latitude 26.61°; Longitude 92.78°, Elevation=82m), Tezpur, Assam, with the installation of several geophysical instruments collecting data simultaneously portray an opportunity towards identification of seismic induced precursory signatures<sup>2,3,4,5</sup>. The Multifractal detrended fluctuation analysis (MF-DFA) is a very modern technique which highlights large information hidden in a time series data. The MF-DFA technique is a well modified version of the fractal analysis. The MF-DFA technique was applied and scrutinized to estimate and identify the complex underlying phenomena in the geomagnetic total field intensity<sup>6,7</sup>. The MF-DFA was carried for complex geomagnetic total field intensity time series to quantify the degree of multifractality and to investigate the correlation

with earthquake occurring in the vicinity of MPGO, Tezpur which is located in a highly tectonically strained and seismically active region. On 12<sup>th</sup> September, 18, a shallow depth (13 km) earthquake (event) of Mw~5.5, occurred at Kokrajhar, Assam on 10:20:49 (IST). The anomalies and multifractal analysis of geomagnetic total field intensity ( $B_{\text{Total}}$ ) prior to Mw~5.5 event was investigated in Multiparametric Geophysical Observatory, Tezpur. The investigation also manifested some non-linear features which probably evinced the anomalies to be seismic induced.

## 2 Methodology

Overhauser Magnetometer (GSM-19W v7.0) is installed and into operation in MPGO, Tezpur to acquire the geomagnetic total field intensity. The sensors are mounted on a pole with a receiver unit with inbuilt memory (Base Station: 2,708,821 readings) for data acquisition. The geomagnetic total field intensity is continuously monitored at sampling rate of 5 second. The arrangement is set up in remote location inside an iron free insulated doom house to minimize the noise from external sources. The GSM-19W v7.0 has sensitivities of 0.015 nT /  $\sqrt{\text{Hz}}$  @ 1 sample/second or better with a resolution of resolution (0.01 nT).

\*Corresponding author: (E-mail: saurabh\_23@gmail.com)

In the manuscript we have applied and adopted the method of MF-DFA as described by Kantelhardt<sup>8</sup>. If  $x_k$  is a time series of length  $N$  the profile can be calculated as,

$$Y(i) = \sum_{k=1}^i [x_k - \langle x \rangle] \quad \dots(1)$$

where  $i=1, \dots, N$  and  $\langle x \rangle$  the mean of the time series.

The  $Y(i)$  profile is divided into non overlapping segments of equal length as,

$$N_s = \text{int}(N/S) \quad \dots(2)$$

The length  $N$  may not be exact multiple of time scale and so that short part at the end does not get omitted, the procedure is repeated from the opposite end. Therefore  $2N_s$  segments are acquired altogether.

The local trend is then calculated for each of the  $2N_s$  segment by applying least square fit to the series and then the variance is determined by:

$$F^2(s, v) = 1/s \sum_{i=1}^s \{Y[(v-1)s+i] - y_v(i)\}^2 \quad \dots(3)$$

For each segment  $v$ ,  $v=1, \dots, N_s$

$$F^2(s, v) = 1/s \sum_{i=1}^s \{Y[N - (v - N_s)s + i] - y_v(i)\}^2 \quad \dots(4)$$

Different types of fittings procedure e.g. linear, quadratic, cubic, or higher order polynomials can be used (conventionally called DFA1, DFA2, and DFA3.....). The average of the entire segments to obtain  $q^{\text{th}}$  order fluctuating function is estimated as:

$$F_q(s) = s \{1/2N \sum_{v=1}^{2N_s} [F^2(s, v)]^{q/2}\}^{1/q} \quad \dots(5)$$

Here in the case except zero,  $q$  can take any real value. To determine how the generalized  $q$  dependent fluctuation function  $F_q(s)$  on time scale  $s$  for different  $q$  values. The procedure is now repeated for different values of the time scale for length of the segment  $v$ . Then to determine the scaling behavior of fluctuating function log-log plots  $F_q$  versus  $s$  for each value of  $q$  is analyzed. The exponents  $h(q)$  can be obtained by observing the slope of the log-log plot of  $F_q(s)$  versus  $s$ . If the time series  $x_k$  are long-range power-law correlated,  $F_q(s)$  increases for large value of  $s$ , as a power-law:

$$F_q(s) \sim s^{h(q)} \quad \dots(6)$$

In general the exponent  $h(q)$  depends on  $q$ . In monofractal time series  $h(q)$  is independent of  $q$  and  $F^2(s, v)$  is identical for all segments  $v$  and are dominant by identical scaling behavior<sup>2</sup>. If a negative Hurst exponent is obtained, the time series is integrated before applying MF-DFA technique to it.

To quantify the multifractality in a time series spectrum,  $D_q$  is derived by mathematical relation between  $h_q$  and classical scaling exponent  $\tau(q)$  as below:

$$\tau(q) = qh(q) - 1 \quad \dots(7)$$

The Holder exponent (singularity strength) can be obtained by Legendre transform of  $\tau(q)$ <sup>9</sup> as:

$$h_q = d\tau/dq \quad \dots(8)$$

and the multifractal spectrum  $D_q$  by:

$$D_q = qh_q - \tau_q \quad \dots(9)$$

### 3 Result and discussion

Multifractal Detrended Fluctuation Analysis (MF-DFA) is a common tool to reveal the nature of the scaling and fractionality of a natural or computer generated process. MF-DFA is an arithmetical algorithm intended to determine the stochastic process self-similarity. The algorithm inspects the relation among the diffusion of the process and its propagation in space or time. Auto-regressive and stochastic processes with different power-law scaling will diffuse with different rates. The Fluctuation Analysis (FA) provides a method to reveal these correlations, however fails in the presence of trends in the time series data. Detrending the data using polynomial fittings (DFA) permits to reveal exclusively the relation between the inherent fluctuations and the time scaling of a process, thus circumventing the impact of non-stationarity in the data. Similarly, other methods like empirical mode decomposition or moving average windows are viable options of data detrending. Another problem is that a process might be driven by more than one time scale and can be removed either with local polynomial fittings or EMD. Furthermore, a stochastic process might be of a monofractal/multifractal in nature. Studying a range of power variations of Detrended Fluctuation Analysis one extends into MF-DFA, which allows to scrutinize the fractality of the data by power variations comparison, *i.e.* multifractal spectrum.

The daily average  $B_{\text{Total}}$  during the period of investigation (01/09/18 – 15/09/18) was 48725.6 nT with a standard deviation of 11.73 nT. An anomalous increase (48761.4 nT) in the  $B_{\text{Total}}$  6 days prior to the event was observed. The  $B_{\text{Total}}$  started decreasing gradually from its highest peak anomaly (48759.42 nT) and accomplished the lowest value (48670.21 nT), after 3 days and it started increasing to attain its previous state/trend of fluctuation again till the event occurred Fig 1(a). There was a small

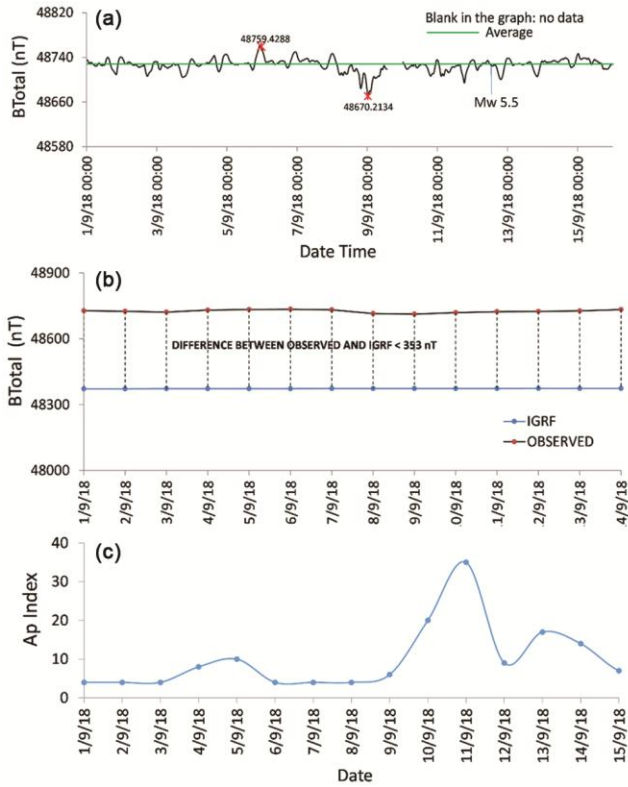


Fig. 1 — (a) Plot showing hourly variation of observed  $B_{Total}$  in MPMO, Tezpur. The highest and lowest anomaly is represented by star along with its values (nT) It is clearly visible  $B_{Total}$  started decreasing gradually from its highest peak anomaly (48759.42 nT) and accomplished the lowest bottom value (48670.21 nT) after 3 days and again it started increasing to attain its previous state of fluctuation till the event occurred, (b) Plot showing the estimated reference field (IGRF-12) and the observed  $B_{Total}$  (average small difference of <353 nT) during the investigation period and (c) The plot representing the Ap index values showing the Ap index < 35 during the investigation time period when the anomalies were observed.

difference of  $\leq 353$  nT between the observed  $B_{Total}$  and geomagnetic reference IGRF-12 model Fig 1(b) for the investigation site. The daily rate change during the anomaly period (from 06/09/18) ranged from -6.76 to 17.05 nT. However, it was observed that 14 -15 days prior to the anomaly period the average daily rate change ranged between -9.27 to 3.64 nT *i.e.* the  $B_{Total}$  manifested a decrease and increase of about -2.52 to 13.41 nT between the anomaly and prior anomaly period. When  $Ap > 29$  it is considered as storm, a minor storm when  $29 < Ap < 50$ , a major storm when  $50 \leq Ap < 100$  and a severe storm when  $Ap \geq 100$ . It was observed that the Ap index was  $\leq 35$  Fig 1(c) during the investigation period when the anomaly in the earth's  $B_{Total}$  was observed.

The  $\log_2(F_q)$  vs.  $S$  were observed by applying linear detrend (DFA1) for a scale of  $2^{10}$  (1024) for

different values of  $q = -5, 0, +5$  to evince whether the  $B_{Total}$  time series is multifractal, monofractal or white-noise. The different values of  $q = -5, 0, +5$  is represented by black, grey and pink dot and the regression fit by the respective colour solid line for  $B_{Total}$  Fig 2(a). In case of monofractal or whitenoise time series, the Hurst exponent ( $h_q$ ) has identical values (*i.e.*  $h_q = H(\text{constant})$ ) for different  $q$  values<sup>11</sup>. It was seen that the  $B_{Total}$  had Hurst exponent with non-identical values for different values of  $q$  which evinces  $B_{Total}$  time series to be multifractal in nature. The first order polynomial detrend (DFA1: linear detrend) was applied to 8192 data points of  $B_{Total}$  (scale  $2^{13}$ ) for 11/09/18 ( $T_{Day\ one}$ : Multifractal spectrum of  $B_{Total}$  for a day prior to the event), for 12/09/18 ( $T_{Event\ day}$ : Multifractal spectrum of  $B_{Total}$  during the day when event occurred) and for surrogate  $B_{Total}$  ( $T_{Surrogate}$ : Multifractal spectrum of surrogate  $B_{Total}$ ) by applying Iterated Amplitude Adjust Fourier Transform (IAAFT). The multifractal spectrum  $T_{Day\ one}$ ,  $T_{Event\ day}$  and  $T_{Surrogate}$  is represented by red, blue and green coloured curves (spectrum) respectively in Fig 2(d). It is discernible that the values of the generalized Hurst exponent ( $h_q$ ) for  $T_{Day\ one}$ ,  $T_{Event\ day}$  is nonlinear function of  $q$  ( $-5, 0, +5$ ) which clearly reveals that time series exhibit multiscaling properties Fig 2(b)<sup>10</sup>. The value of  $h_q$  for different values of  $q = -5, 0, +5 > 0.5$  substantiate that the  $T_{Day\ one}$  and  $T_{Event\ day}$  time series is persistent time series Fig 2(b) *i.e.* an increase or decrease is probably to be followed by another decrease or increase respectively in the short term. It is visible that  $T_{Day\ one}$  and  $T_{Event\ day}$  time series to be multifractal as  $t_q$  has non-linear  $q$ -dependencies (curved  $q$ -dependencies) which results in different  $h_q$ <sup>4, 12, 13</sup> with large arc multifractal spectrum represented in Fig 2(c). The value of  $h_{qmax} - h_{qmin}$  for  $T_{Day\ one}$ ,  $T_{Event\ day}$  and  $T_{surrogate}$  was calculated to be 0.6571, 0.9009 and 1.0012 respectively. The multifractal spectrum produced by  $T_{Day\ one}$  time series was found to be right skew since value of  $b > a$  Fig 2(d); red coloured spectrum) signifying finer (coarser) structures in the data and direct relevance to the shape of Hurst exponent ( $h_q$ ) plots, plotted as a function of  $q$ <sup>14</sup> also denoting relatively strongly weighted high fractal exponents corresponding to fine structures<sup>15</sup>.

The  $T_{Day\ one}$  MF-DFA along with its surrogates time series were carried out to study the degree of multifractality by comparing it with the surrogate time series Fig 2(d); green coloured spectrum). The width of the spectrum *i.e.* ( $h_{qmax} - h_{qmin}$ ) observed was

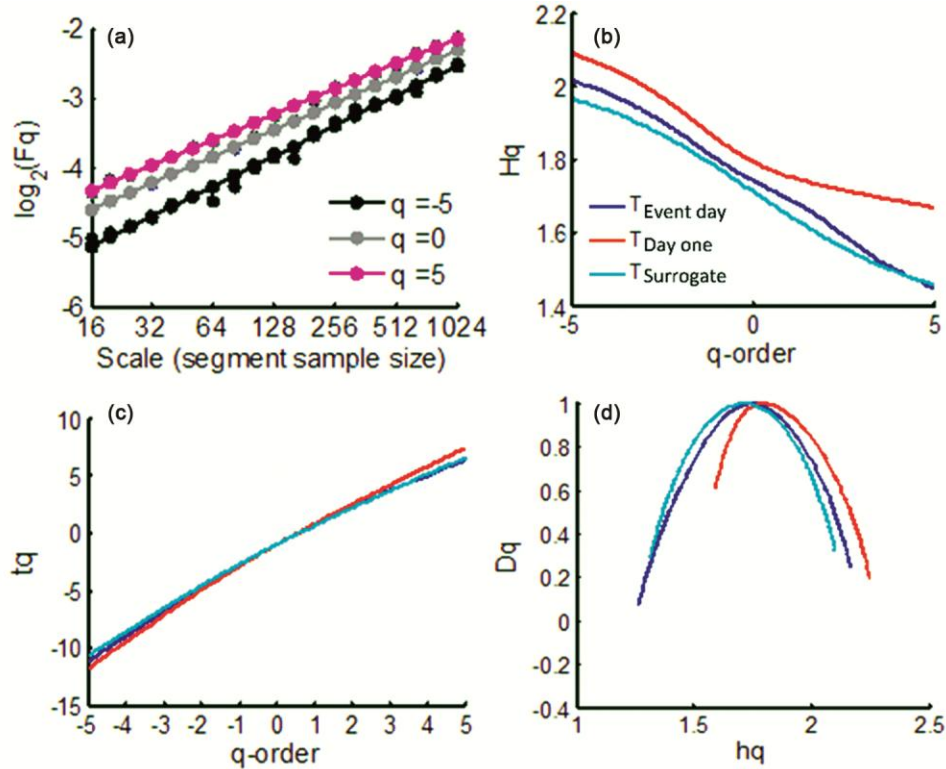


Fig. 2 — (a) Plot showing the  $\text{Log}_2(F_q)$  with scale  $2^N$  ( $N=4, \dots, 10$ ) for different values of  $q=-5, 0, +5$ . The value of  $\text{Log}_2(F_q)$  mismatches for different value of  $q$  indicating the  $B_{\text{Total}}$  to be persistent time series in nature, (b) Plot showing generalized Hurst exponent ( $h_q$ ) for different  $q$  values ( $q_{\min}=-5$  to  $q_{\max}=+5$ ) of  $B_{\text{Total}}$ , (c) Plot showing  $t_q$  for different  $q$  values ( $q_{\min}=-5$  to  $q_{\max}=+5$ ) of  $B_{\text{Total}}$  for and (d) Multifractal spectrum of  $B_{\text{Total}}$  on  $T_{\text{Event day}}$  (Blue line),  $T_{\text{Day one}}$  (Red line) and  $T_{\text{Surrogate}}$  (Green line) respectively.

$W_{\text{Day one}} < W_{\text{Event day}} < W_{\text{Surrogate}}$  (width of  $T_{\text{Day one}}$ ,  $T_{\text{Event day}}$  and  $T_{\text{Surrogate}}$ ) which suggest the degree of multifractality in  $T_{\text{Surrogate}}$  is visibly to some extent stronger than  $T_{\text{Event day}}$  and  $T_{\text{Day one}}$  time series. The degree of multifractality of  $T_{\text{Event day}}$  was observed to be stronger than  $T_{\text{Day one}}$ . This also suggests that the multifractality of  $T_{\text{Day one}}$  and  $T_{\text{Event day}}$  time series is not from source type long range correlation or sourced from broad probability density function. The value of  $h_{q_{\max}}$  (holder exponent) evince that the  $T_{\text{Day one}}$  time series pattern is more irregular in nature (since  $h_{q_{\max}} \gg 0$ ) with longer tail (left or right) evincing more heterogeneity in the data distribution<sup>3</sup>. On the other hand the multifractal spectrum for  $T_{\text{Event day}}$  was observed to have shorter left tail and left skewed spectrum evincing less heterogeneity in the data distribution slightly with higher slope than  $T_{\text{Day one}}$  which also means the multifractality of the time series is largely due to low value distribution<sup>12, 15, 16</sup>. The multifractal spectrum of  $T_{\text{Day one}}$  has been observed to have a long right tail which relates it to greater heterogeneity and uniformity of low values distribution.  $T_{\text{Event day}}$  exhibited multiscaling property but contradictorily the multifractal spectrum for  $T_{\text{Event}}$

day was observed to have width  $W_{\text{surrogate}} > W_{\text{Event day}} > W_{\text{Day one}}$  Fig 2(d) which suggest the degree of multifractality visibly got stronger than  $T_{\text{Day one}}$  but weaker than  $T_{\text{Surrogate}}$  time series on the day when the event occurred Fig 2(d). Multifractality of  $T_{\text{Event day}}$  Fig 2(d) time series evinced to get stronger than  $T_{\text{Day one}}$  Fig 2(d). Further on the  $T_{\text{Event day}}$  multifractal spectrum is not similar (right skewed spectrum with short left tail) to the  $T_{\text{Day one}}$  and  $T_{\text{Surrogate}}$  spectrum which signifies that  $T_{\text{Event day}}$  is dependent on the broadness of the probability density functions<sup>9</sup>. A significant variation in the multifractal spectrum was observed between  $T_{\text{Day one}}$  and  $T_{\text{precursory day}}$ . It was fascinatingly observed that the multifractality of  $B_{\text{Total}}$  when the event occurred got stronger than the multifractality of  $T_{\text{Day one}}$  and was sourced from low values distribution.

#### 4 Conclusion

An anomalous increase (48761.4 nT) in the  $B_{\text{Total}}$  6 days prior to the event was observed. The  $B_{\text{Total}}$  started decreasing gradually from its highest peak anomaly (48759.42 nT) and accomplished the lowest value (48670.21 nT), after 3 days and again it started

increasing to attain its previous state/trend of fluctuation till the event occurred. The daily rate change during the anomaly period ranged from -6.76 to 17.05 nT. Fascinatingly it was observed that 14-15 days prior to the anomaly period the average daily rate change ranged between -9.27 to 3.64 nT i.e. the  $B_{\text{Total}}$  manifested a decrease and increase of about -2.52 to 13.41 nT between the anomaly and prior anomaly period. The multifractal analysis identified the various complex underlying phenomena in the geomagnetic total field intensity time series. Based on the analysis and observations it evinces that that time series exhibit multiscaling properties and is persistent in nature. The analysis evinced that the time series has finer (coarser) structures in the data and direct relevance to the shape of Hurst exponent ( $h_q$ ) plots, plotted as a function of  $q$  also denoting relatively strongly weighted high fractal exponents corresponding to fine structures. It was fascinatingly observed that the multifractality of  $B_{\text{Total}}$  when the event occurred got stronger than the multifractality of  $T_{\text{Day one}}$  (a day prior to the earthquake) and was sourced from low values distribution. The investigation also evinced the multifractality in  $T_{\text{Day one}}$  and  $T_{\text{Event day}}$  time series was not from source type long range correlation or sourced from broad probability density function. The investigation also manifests some non-linear features which probably evinces the anomalies observed were to be seismic induced.

### Acknowledgements

We thank Ministry of Earth Science, Govt. of India for the financial support provided. We also thank Director CSIR-NEIST, Jorhat, Assam for giving necessary permission to publish the work manifold.

Author C. Dey thankfully acknowledges the Council of Scientific and Industrial Research (CSIR), Government of India, for the award of CSIR SRF vide File No: 31/0025(11858)/2021-EMR-I.

### References

- 1 BIS, Indian standard criteria for earthquake resistant design of structures, 1 (2002).
- 2 Chetia T, Baruah S, Dey C & Sharma S, *Geomat, Natur Hazards Risk*, 11 (2020) 1093.
- 3 Chetia T, Sharma G, Dey C & Raju P L, *Geotectonics*, 54 (2020) 83.
- 4 Dey C, Baruah S, Rawat G, Chetia T, Baruah S & Sharma S, *Phys Earth Planet Inter*, 318 (2021) 106759.
- 5 Dey C, Baruah S, Choudhury B K, Chetia T, Saikia S, Sharma A & Phukan M K, *Annal Geophys J*, 64 (2021) SE330.
- 6 Seddik Kasdi A, Bouzid A, Hamoudi M & Abtout A, *In EGU General Assembly Conference Abstracts*, (2021) EGU21.
- 7 Alam A, Wang N, Petraki E, Barkat A, Huang F, Shah M A, Cantzos D, Priniotakis G, Yannakopoulos P H, Papoutsidakis M & Nikolopoulos D, *Pure Appl Geophys*, 178 (2021) 3375.
- 8 Wu J G & Lundstedt H, *Geophys Res Lett*, 23 (1996) 319.
- 9 Kantelhardt J W, Zschiegner S A, Koscielny-Bunde E, Havlin S, Bunde A & Stanley H E, *Physica A: Statist Mech Appl*, 316 (2002) 87.
- 10 Albert-László Barabási & Tamás Vicse, *Phys Rev A*, 44 (1991) 2730.
- 11 Ihlen E A, *Front Physiol*, 3 (2012), 141.
- 12 Ihlen E A & Vereijken B, *Human Movem Sci*, 32 (2013) 633.
- 13 Subhakar D & Chandrasekhar E, *Physica A: Statist Mech Appl*, 445 (2016) 57.
- 14 Baranowski P, *Facce Macsur Rep*, 5 (2015) 5.
- 15 Pavon-Dominguez P, Jimenez-Hornero F J & de Rave E G, *Atmos Pollut Res*, 4 (2013) 229.
- 16 Sarker A & Mali P, *Chaos, Solit Fract*, 151 (2021) 111297.